Extracting ionospheric Measurements from GPS in the Presence of Anti-Spoofing

Brian D. Wilson and Anthony J. Mannucci

Jet Propulsion 1 aboratory, California Institute 01' Technology
Pasadena, CA 91109

Biographies

Brian Wilson, a member of the GPS Network Operations Group at the Jet Propulsion Laboratory in Pasadena, CA, has been studying the ionosphere using Faraday rotation and GPS data for five years. He is the Cognizant Design Engineer of the current operational ionosphere calibration software for the Deep Space Network, which uses GPS data from multiple sites to correct navigation radiometric data for ionospheric delay effects. He continues to pursue efforts to improve the calibration system and validate its accuracy by comparisons with independent ionosphere measurements such as Very Long Baseline Interferometry and the TOPEX dual-frequency altimeter. He is currently involved in producing sub-hourly global ionospheric maps using GPS data from 50+ world-wide sites and validating their accuracy.

Anthony J. Mannucci is a member of the technical staff in the GPS Network Operations Group at the Jet Propulsion Laboratory in Pasadena, CA. He has spent the last four years developing and characterizing ionospheric calibration systems for deep space tracking and Earth-orbiter satellite applications. He has over ten years of experience developing high accuracy measurement techniques in a variety of technical areas. Currently, he is focusing on increasing the accuracy of GPS-based global ionospheric maps by improving the algorithms and estimation strategy.

Abstract

Line-of-sight ionospheric measurements derived from differencing dual-frequency Global Positioning System ((i)PS) pseudorange data are corrupted by instrumental biases in both the receiver and GPS satellite transmitters due to hardware delays in the L1 and L2 signal paths. Hardware calibration of the instrumental delay is possible for some types of receivers (e. g., Allen Osborne Associate's Rogue SNR-8), but the satellite biases must be estimated using a remote technique. Ignoring the satellite (receiver) biases when computing line-of-sight TEC measurements from GPS observables may result in an error of ±9 (±30) TECU (1 TEC unit = 10^{16} electrons/meter^2 = 0.3S nanoseconds of differential delay).

Using a global ionospheric shell model to fit GPS-based ionospheric delay data from a worki-wide network of 50+ receivers, we can simultaneously estimate a global ionospheric map, satellite biases for the entire GPS constellation, and receiver biases for all the uncalibrated receivers. The uncertainty in the resulting estimates of the satellite biases is a dominant error source in extracting line-of-sight TEC measurements from GPS observables. We present the results of daily fits of satellite biases over a period spanning 20 months from Jan. 1993 through Aug. 1994. Seven separate time periods each consisting of 10-12 consecutive days were processed. The day-to-day variability of the estimates has been computed in an effort to assess their precision. Before anti-spoofing (AS) encryption of the GPS ranging code, the estimated satellite biases exhibited a day-to-day standard deviation of 0.6 nanoseconds or 1.7 TECU. With the advent of AS encryption, the pseudorange observable exhibits a lower signal-to-noise ratio, but the day-to-day reproducibility of the biases has not changed significantly. This preliminary study indicates that AS has not had a significant impact on our estimates of the satellite biases. The current satellite bias estimates (with AS on) are consistent with the pre-AS values to a precision of 0.6 ns or 1.7 TECU.

Introduction

line-of-si@l ionosphere measurements derived from differencing dual-frequency GPS delays are corrupted by instrumental biases in both the receiver and GPS satellite transmitters. The instrumental bias is the difference between the two dispersive delays introduced by the analog hardware in the L1 and L2 signal paths. The line-of-sight differential delay between a GPS receiver and satellite can be modeled as the sum of a receiver bias, a satellite transmitter bias, and the actual line-of-sighl ionospheric total electron content (TEC). Our experience with hardware calibrations from the Rogue SNR-8 receiver (Allen Osborne Associates) indicate that the bias

values are typically in the range ±10 nanoseconds (ns) of differential delay and have a month-to-month stability of 0.2 ns when the receiver is in a temperature stabilized environment. Estimates of the satellite transmitter biases indicate they lie in the range of ±3 ns or ±9 TECU (1 ns of differential delay at L band = 2.85 TECU). Therefore, obtaining accurate absolute measurements of TEC from GPS data requires that these bias values be from the line-of-sight measurements.

Numerous studies have reported satellite bias values derived from various estimation strategies based on the GPS data [B. D. Wilson, *et al*, 1993; G. E. Lanyi and T. Roth, 1988; D. S. Coco, *et al*, 1991; E. M. Gaposchkin and A. J. Coster, 1993; E. Sardón and L. Wanninger, 1993; S. B. Gardner, 1993; and others]. All of these studies were completed before the GPS Block II constellation became operational on Jan. 31, 1994 which resulted in the encryption of the precise pseudorange code (anti-spoofing). The purpose of this paper is to investigate how the advent of anti-spoofing (AS) has affected the estimates of the satellite biases and, consequently, the accuracy of line-of-sight TEC measurements computed from GPS observables.

Almost all of the bias estimates reported by other groups have been based on data from a single GPS receiver. Single-site techniques have also been used at JPL as part of an operational ionosphere calibration system for NASA's Deep Space Network [Lanyi and Roth, 1988]. Since 1992, we have used a more robust strategy for bias estimation by processing data from several receiver sites simultaneously to produce global ionospheric maps (GIM), which are maps of vertical total electron content over the entire globe [Mannucci *et al.* 1993; Wilson *et al.*, 1994]. A multi-site technique allows us to bring much more data to bear on the bias estimation problem. Since the formation these maps involves the simultaneous estimation of ionospheric delay and the receiver and satellite biases, we have found that the tasks of estimating the biases and modeling the ionosphere are intertwined. Improvements in our ionospheric fitting and mapping techniques have led to improved bias estimates as evidenced by reduced day-to-day scatter in the bias values [Wilson, *et al*, 1993].

TEC model	2-D shell model approximation
Vertical TEC fit to	Triangular grid, 642 vertices
Support of the basis set	Local, interpolation within triangles
Spatial resolution	8 degrees in latitude & longitude
Temporal resolution	30-60 minutes; can track short-term changes
Parameter estimation	TEC at each vertex is treated as a random walk (stochastic parameter)
Day-to-day scatter of estimates of the [illegible]	0.6 ns or 1.7 TECU before AS

Figure 1 - A summary of the parameters characterizing the TRIN model.

Ionosphere Model and Estimation Strategy

The satellite bias estimates are derived from a global ionospheric mapping technique which will be summarized briefly here. The details of the model, known as "TRIN", are described in Mannucci, *et al*, 1993 and Wilson, *et al*, 1993. Briefly, the Earth's vertical electron content distribution is assumed to arise from a thin "shell" of ionization at a fixed height of 350 km. The global ionospheric spherical shell is tessellated with 1280 triangles (8 degrees on a side) and the TEC at each of 642 vertices is estimated using local linear interpolation of the GPS data within the triangles. The TEC at each vertex is treated as a random walk stochastic parameter and is updated every 60 minutes (more frequent updates are possible). Thus, the TRIN model produces a global snapshot of vertical TEC every hour. A summary of the important characteristics of the TRIN model appears in Figure 1.

Each line-of-sight measurement between a GPS receiver and satellite intersects the ionospheric shell at a single latitude and longitude. The line-of-sight TEC is assumed to be related to the vertical TEC at the intersection point by an elevation mapping function M(E), which is the simple geometric slant ratio at the shell height h:

$$M(E) = \{1 - [\cos E / (1 + h/R)]^2\}^{-1/2} \qquad (1)$$

where E is the elevation angle and R is the radius of the earth. The measured differential delay between the *i*th receiver and the *j*th GPS satellite τ^{LOS}_{ij} can be modeled by the following expression:

$$\tau^{LOS}_{ij} = \tau^{r}_{i} + \tau^{s}_{j} + K\, M(E)\, TEC(\theta_{ij}, \phi_{ij}) \qquad (2)$$

where τ^{r}_{i} is the instrumental bias for the *i*th receiver, τ^{s}_{j} is the bias for the *j*th satellite transmitter, K (= 0.35) is a constant relating differential delay at L band in nanoseconds to ionospheric TEC in TECU, M(E) is the

elevation mapping function, and TEC(θ_{ij} , ϕ_{ij}) is the vertical TEC at shell latitude θ_{ij} and shell longitude ϕ_{ij} . A Kalman-type filter is used to simultaneously estimate the vertical TEC over the entire globe along with the satellite biases for the entire GPS constellation and receiver biases for the uncalibrated receivers.

Since the receiver and satellite biases are always paired for each measurement, it is not possible to solve for the receiver and satellite biases separately unless additional assumptions are made. In this case, we used the measured receiver bias value at the GPS station in Madrid to set the levels for all the remaining biases. Since the data from the multiple receiver sites overlap on the ionospheric shell, data from the entire global network contributes to the estimation of the satellite and receiver biases and allows absolute levels to be determined when knowledge of only a few receiver biases is available.

Results and Discussion

When AS is on, the GPS precision ranging code (P-code) is encrypted and the receivers in the GPS global network use a cross-correlation technique to generate the pseudorange and carrier phase observables. (The global network data processed here is obtained from Allen Osborne Associates Rogue SNR-8 and TurboRogue SNR-8000 receivers). These P-codeless tracking observables exhibit larger noise than the P-code observables, particularly at low elevations. Figure 2 shows differential pseudorange data (P2 - P1) from a Rogue receiver which is tracking the same satellite simultaneously in two channels: one using the P-code and the other using the cross-correlation technique (P-codeless mode). The level of the P-code data has been shifted in order to separate the two curves for visibility. The scatter of the P-codeless data is a factor of 2 to 10 times larger than the scatter of the P-code data, depending on the elevation. More modern receivers, such as TurboRogue and Ashtech, produce P-codeless data which is more precise than that from the Rogue receivers. However, since the global receiver network which we use at JPL to produce the global ionospheric maps contains a significant number of Rogue receivers, we find it advantageous to process this data in spite of the higher noise levels.

Fortunately, the ionospheric measurements do not depend solely on the pseudorange noise since pseudorange-leveled carrier phase is used as the TEC observable [see Mannucci, *et al.*, 1993]. To form this observable, the frequency-differenced carrier phase is adjusted by a constant value determined for each phase-connected arc of data. The frequency-differenced phase data is a biased measure of total electron content but has a noise level 2-3 orders of magnitude below the pseudorange data.

Formation of the TEC observable can be described as follows. Let P_i be the ith measurement of frequency-differenced pseudorange (P2 - P1) in a phase connected data arc consisting of N points. If Φ_i is the ith frequency-differenced phase measurement (L1 - L2), then a leveling constant C for the arc is computed as follows:

$$C = \frac{1}{N}\sum_{i=1}^{N}(P_i - \Phi_i) \qquad (3)$$

The TEC observable T_i is formed by adding this constant to the phase measurements:

$$T_i = \Phi_i + C \qquad (4)$$

Setting the level of the carrier phase data using the pseudorange takes advantage of the high precision of the phase data. The precision of the TEC observable exceeds that of the psedorange data alone since many points along the arc contribute to the leveling constant. The same leveling procedure can be used for encrypted and unencrypted data because in both cases the frequency-differenced pseudorange and carrier phase data are available. However, when AS is on, the precision of the pseudorange data is severely degraded at low elevations. Therefore, we currently impose an elevation cutoff of 30 degrees for encrypted data and 20 degrees for unencrypted data.

A measure of the precision of the TEC observable can be obtained by calculating the root-mean-square difference between the leveled carrier phase and the pseudorange data. If the pseudorange noise statistics were dominated by white noise, the precision of the TEC measurement would be smaller than this RMS difference by a factor equal to the square-root of the number of points in a phase-connected arc. For unencrypted data and an elevation cutoff of 20 degrees, the RMS difference averaged over every phase-connected arc in a single day of global network data is typically about 0.7 TECU for data extracted at 6 minute intervals. For encrypted data, we have used an elevation cutoff of 30 degrees, yielding an RMS value of about 2.4 TECU. These numbers apply exclusively to Rogue receivers; the TurboRogue receivers exhibit RMS differences which are about 2-3 times smaller.

In order to investigate the effect of anti-spoofing on the satellite bias estimates, we compared the bias estimates from four different periods: March 12-23, 1993 and August 6-17, 1993 when AS was off, and February 11-19, 1994 and August 17-26, 1994 when AS was on. The ionosphere was relatively quiet, as measured by the global geomagnetic index Ap, in both Aug. '93 (mean Ap = 8 over 12 days) and Aug. '94 (mean Ap = 6), and moderately disturbed in Mar. '93 (mean Ap = 25) and Feb. '94 (mean Ap = 28). For each period, daily fits were performed in which the biases were assumed to be constant over the entire day and the ionosphere at each of the vertices was updated every hour. The absolute level

of the satellite biases was set by constraining one of the receiver biases to its hardware calibration value.

One way to assess the precision of the estimated satellite biases is to examine the variation in the daily estimates over each 10-12 day period. These variations consistently exceed the formal errors computed by the least-squares filter, indicating the presence of unmodeled systematic effects, or actual daily fluctuations in the bias values themselves. Assuming the biases are actually constant over several days, the best estimate of the satellite biases might be obtained by using the average over many days. In this case, the daily scatter in the bias values provides an indication of how the mismodeling affects the estimates from day to day.

Figure 3 illustrates the day-to-day scatter for two typical satellite biases (PRN#'s 13 and 15) during the four periods. The levels of the biases have been adjusted arbitrarily in order to separate the lines for visibility. Note that the scatter is smaller in Aug. '94 when the ionosphere was quiet (but AS was on) than in both Mar. '93 (AS off) and Feb. '94 (AS on) when the Ap index indicates greater geomagnetic activity. Also, the scatter for Aug. '94 (AS on) is slightly smaller than that for Aug. '93 (AS off). Thus, the day-to-day reproducibility appears to depend more strongly on the state of the ionosphere than on whether AS was active. The other feature of interest in Figure 3 is that the bias estimates sometimes move up and down in unison. This behavior suggests that systematic ionospheric mismodeling contributes to the scatter.

Figure 4 gives the complete table of estimated satellite biases for the same four periods. The quoted biases and errors are the averages and standard deviations of 10-12 successive daily values. The combined standard deviation for all of the satellites in each period is 0.93, 0.27, 0.44, and 0.17 ns respectively. The disturbed period, March '93, has the highest level of scatter while both of the quiet August periods have lower levels of scatter. Figure 4 indicates that the use of encrypted data does not gravely impact the precision of the satellite bias estimates, while the presence of more geomagnetically active ionospheric conditions is correlated with increased day-to-day scatter. Moreover, assuming that the satellite biases are actually constant over several days, it is reasonable to expect that as the solar cycle progresses toward the next minimum, the day-to-day reproducibility of the bias estimates should improve. The difference in scatter between August 1993 and August 1994 follows this trend.

The values of the satellite bias estimates did not change significantly when AS became active on January 31, 1994. This fact is evident for the four periods tabulated in Figure 4 and is also true more generally. Using a more extensive set of data, we find that the estimated satellite biases are consistent with a constant value to a precision of about 0.6 ns (one sigma) over periods of longer than one year. Figure 5 shows a plot of selected satellite biases for seven periods in 1993-94 spanning 20 months: January, March, June, and August of 1993 and January, February, and August of 1994. These biases are averages of daily values for a 10-12 day period in each of the seven months. This plot illustrates qualitatively that the satellite biases have not changed significantly during this 20-month period. If the satellites biases are in fact constant over years, then the best estimate might be obtained by averaging daily values over such time scales.

In order to quantify the stability of the satellite bias estimates over the 20 months covered in this study, one can look at the mean, standard deviation, and total variation (minimum to maximum) of the estimates for each of the seven 10-12 day spans. Figure 6 is a plot of the mean of the seven satellite bias estimates covering the 20 month period. The error bars in Figure 6 represent the total variation of these seven estimates. The total variation is less than 1 ns for approximately half of the satellites and the largest variation is 1.6 ns for GPS #19. The standard deviation of the seven estimates is less than 0.4 ns for most of the satellites and the largest standard deviation is 0.6 ns for GPS #29. This suggests that the satellite biases are constant over many months to a precision of 0.6 ns or 1.7 TECU.

Conclusions

The problem of estimating the instrumental biases in the GPS satellites is difficult because one must simultaneously estimate the TEC using an approximate model of the ionosphere. Therefore, it is not surprising to observe that the day-to-day scatter in estimates of the satellite biases appears to be correlated with the level of geomagnetic activity in the ionosphere (as quantified by the Ap index). Also, the day-to-day reproducibility of the bias estimates may be correlated with the general level of the ionosphere which is dropping as the solar cycle progresses toward the next minimum. A definitive answer to the difficult bias estimation problem may require better ionospheric modeling or model-independent methods which make use of additional TEC data types.

The day-to-day reproducibility of the bias estimates does not appear to be a function of whether the GPS observables are extracted in the presence of anti-spoofing or not, so evidently the effect of the noisier P-codeless data is not significant when only data above 30 degrees elevation is used. As a result, the advent of anti-spoofing has not had a significant impact on our ability to monitor the satellite biases implying that the main effect of AS is increased noise in the P-codeless observable.

The values of the satellite biases did not appear to change significantly when AS became active on January 31, 1994. All of the satellite bias estimates covering a 20-month period from January 1993 to August 1994, which spans both non-AS and AS periods, were found to exhibit a standard deviation about the mean of better than 0.6 ns.

This leads us to tentati vely conclude that the satellite biases are constant in time over many months at the level of 0.6 ns or I .7 TECU.

Acknowledgments

This analysis was made possible by the high quality 01' the global GPS data set, the result 01 a collaborative effort involving many people at JPL and at other centers around the world. We also wish to express our appreciation to Ulf Lindqwister, Dah-Ning Yuan, and Tom Runge for helpful discus sions and suggestions. The research described in this paper was performed by the Jet Propulsion Laboratory, California Institute 0 1 Technology, under contract with the National Aeronautics and Space Administration.

References

Coco, D. S., C. E. Coker, S. R. Dahlke, and J. R. Clynch (1991), Variability of GPS Satellite Differential Group D elay Bia ses, *IEEE Transact ions on Aerospace and Electronic Systems*, **27** (6), 931-938.

Gaposchkin, E. M. and A. J. Coster (1993), GPS 1.1-1.2 Bias Determination, Lincoln I aboratory Technical Report 971 (MIT).

Gardner, S. B. (1993), Inverse Least Squares Computations of Vertical TEC Using a Calibrated GPS Ionospheric Receiver, *Proceedings of the Seventh International Ionospheric Effect s Symposium*, J. Goodman, ed., Alexandria, VA, May 1993.

Lanyi, G. and 'T'. Roth (19S8), A comparison 01 mapped and measured total ionospheric electron content using global positioning system and beacon satellite observations, *Radio Sci.*, **23** (4), 483-492.

Mannucci, A. J., B. D. Wilson, and C. D. Edwards (1993) A New Method for Monitoring the Earth's ionospheric Total Electron Content using the GPS Globa I Network, to appear in *Proceedings of the Institute of Navigation GPS-93*, Sa lt Lake Cit y, Utah, September, 1993.

Sardón, E. and L. Wanninger (1993), Comparison of Several Data Sets of the Differential Instrumental Delays of GPS Satellites, Institut für Erdmessung Memo WA-03/93 (Universität Hannover).

Wilson, B. D. and A. J. Mannucci (1993), Instrumental Biases in Ionospheric Measurements Derived from G}'S I Dat a, to appear in *Proceedings of the Institute of Navigation GPS-93*, Sail Lake City, Utah, September, 1993.

Wilson, B. D., A. J. Mannucci, and c D. Edwards (1994), Sill)-dilily northern hemisphere ionospheric maps using an extensive network of GPS receivers, to appear in a special issue of *Radio Science*.

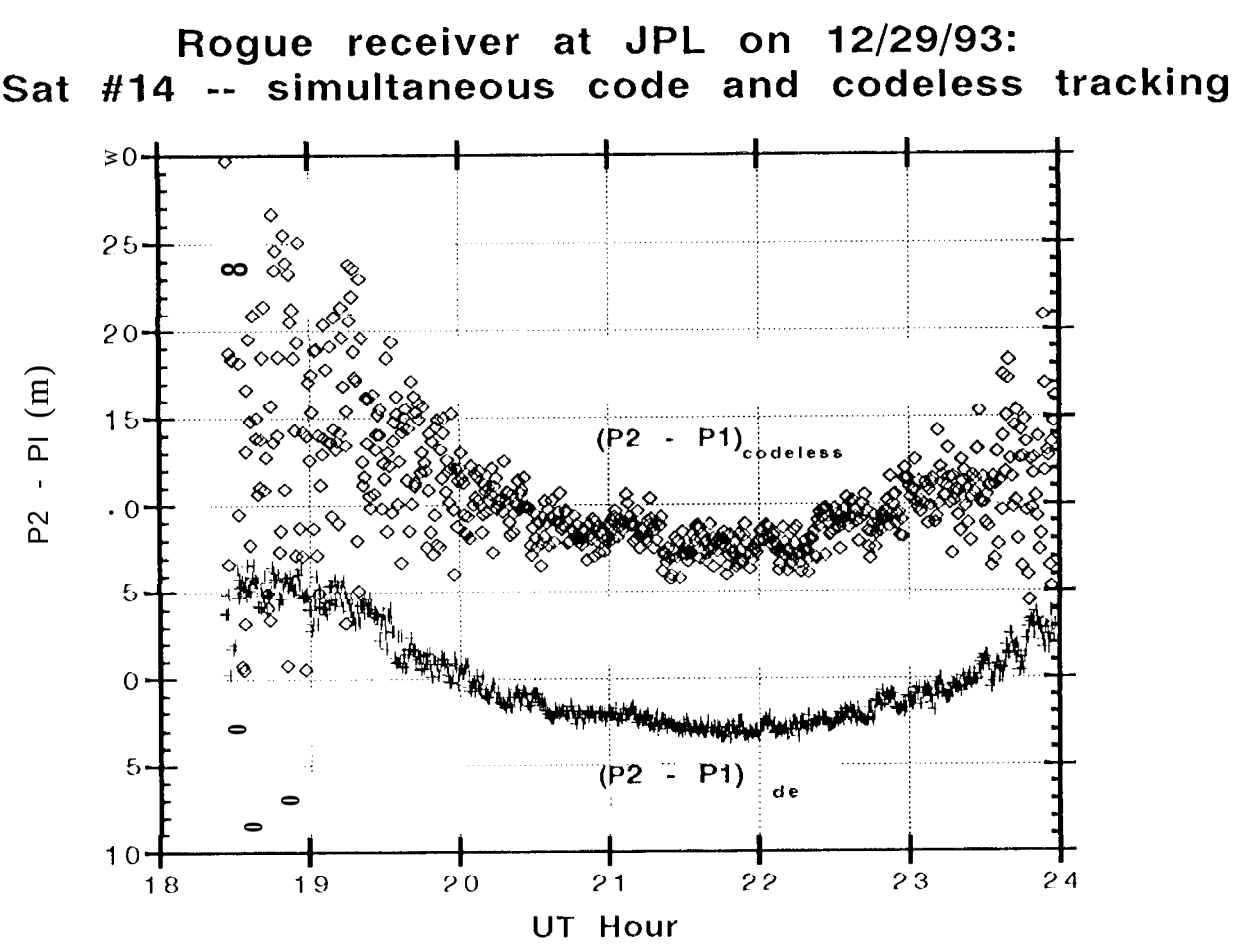

Figure 2 An illustration of the fact that P-codeless differential pseudorange data (P2 - P1) from the Rogue receiver is noisier than P-code mode data by a factor of 2 to 10 depending on the elevation angle. The data are extracted from the receiver at two-minute intervals. Note that the level of the P-code data has been shifted in order to separate the two curves for visibility.

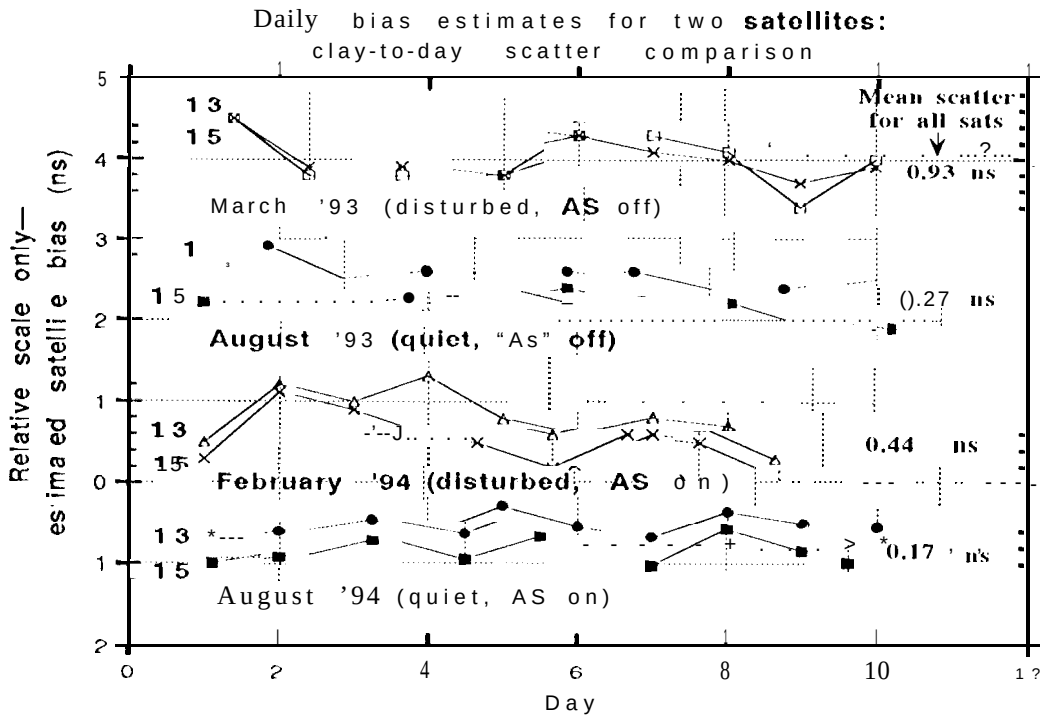

Figure 3 - Day-to-day reproducibility of the satellite bias values plotted over 10 days for four different periods: two with AS off and two with AS on. The levels of the biases have been adjusted arbitrarily in order to separate the lines for visibility. Note that the scatter is not consistently larger for the two AS (codeless data) periods. The day-to-day standard deviation is more strongly a function of the state of the ionosphere than of the presence of AS. Both Aug. '93 and Aug. '94 were quiet periods, while Mar. '93 and Feb. '94 were moderately disturbed.

Satellite GPS #	March '93 Bias (ns)	August '93 Bias (ns)	February '94 Bias (ns)	August '94 Bias (ns)
9	1.0 ± 0.8	0.9 ± 0.3	0.9 ± ().5	
10	2.() ± 1.3	2.1 ± 0.3	2.1 ± ().5	
11	0.7 ± 1.2	0.6 ± 0.2	0.9 ± ()$4	
13	-1.0 ± 1.()	-0.9 ± 0.3	-().5 ± 0.4	-0.4 ± 0.2
14	-().7 ± ().9	-1.() ± ().3	-0.9 ± 1.1	-1.1 ± 0.1
15	-1.5 ± ().7	-1.4 ± 0.3	-0.8 ± ().5	-0.7 ± 0.?
16	-().3 ± 0.8	-().1 ± ().4	0.1 ± 0.4	0.1 ± 0.1
17	-1.4 ± 0.7	-1.3 ± 0.2	-().4 ± ().5	-().4 ± 0.'2
18	-1.5 ± 1.0	-2.5 ± ().9	-2.7 ± ().3	-2.8 i 0.3
19	-1,6 ± 0.9	-1.() ± ().2.	-13 ± 0.4	-1.4 ± 0.4
20	-1.5 ± 1.8	-0.8 ± ().3	-().7 ± ().3	-().7 ± 0.2
21	-1.2 ± ()-/	-1.0 ± ().2	-1.0 ± 0.4	-1.1 ± 0.2
22	-2..4 ± ().6	-?.5 ± 0.2	-1.9 ± 0.4	-1.9 ± 0.1
23	-1.9 ± 0.8	-1.6 i 0.1	-1 .0 ± 0.4	-1.() ± 0.2
24	-1.0 ± 0.8	-().4 ± ().3	-().5 ± ().4	-().3 ± ().1
25	-3.7 ± 1 .()	-3.6 ± 0.3	-4.2 ± ().4	-4.2 ± ().'2
26	-3.2 ± 0.9	-2.9 ± 0.3	-3.5 ± ().4	-3.5 ± 0.2
27	-3.2 ± 1.2	-2.4 ± 0.2	-?.5 ± (),4	-2.5 ± 0.2
28	-3.2 ± 0.9	-3.2 ± 0.2	-3.6 ± ().5	-3.9 ± 0.2
29	-3.3 ± 0.8	-3.5 ± 0.3	-4.6 ± ().3	-4.s ± 0.1
31		-3.3 ± 0.2	-3.4 ± ().4	-3.4 ± 0.2
32	-1.4 ± 0.8	-1.3 ± ().?	-1.3 ± 0.4	-1.4 ± 0.2,
34			-3.5 ± 0.4	-3.2 ± 0.2
35			-2.2 ± ().4	-2.1 ± 0.1
36				-?.2 ± 0.1
37			-1.() ± ().5	-().4 ± 0.2
39			-3.0 ± ().4	-2.5 ± 0.2

Figure 4 Estimated satellite biases for four periods during 1993-94. The quoted values and errors are the mean and standard deviation of 10-12 successive daily estimates.

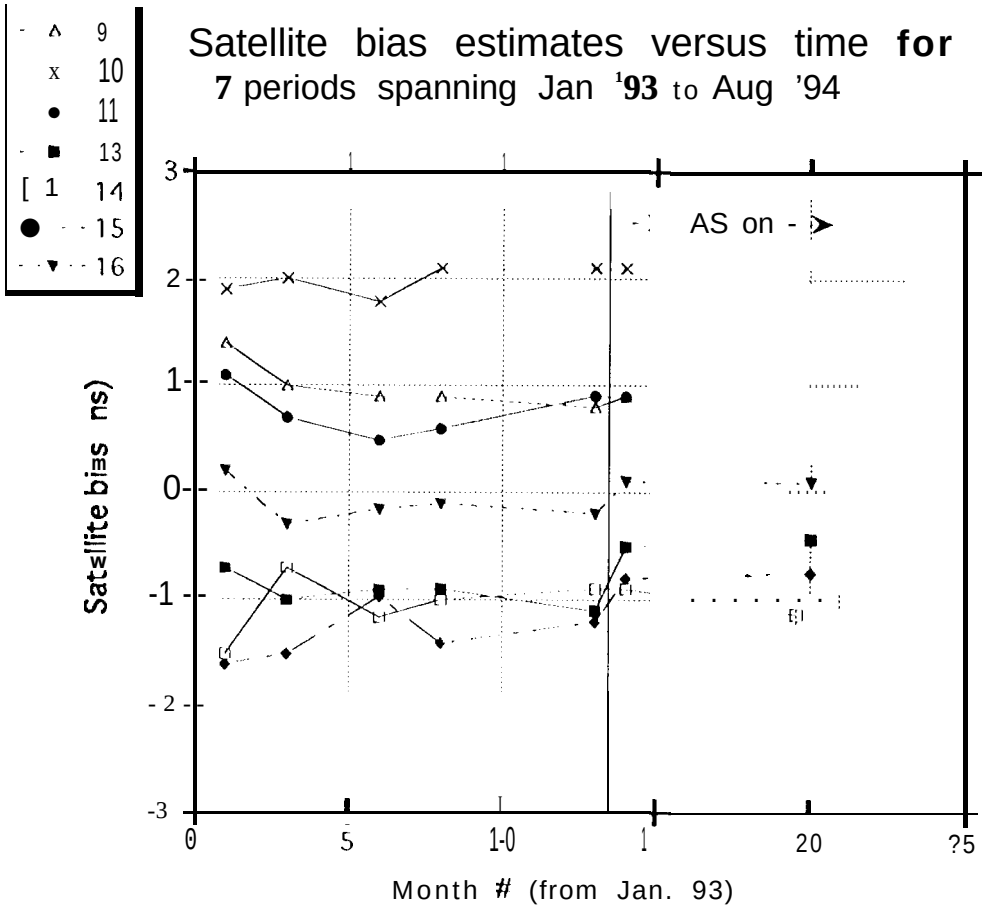

Figure S Plot of selected satellite biases versus time over a period of 20 months. Notice that the biases did not change significantly when AS was turned on (vertical line at month 13). The data are consistent with the claim that the satellite biases are constant in time ill the level of 0.6 ns or 1 .7 TECU.

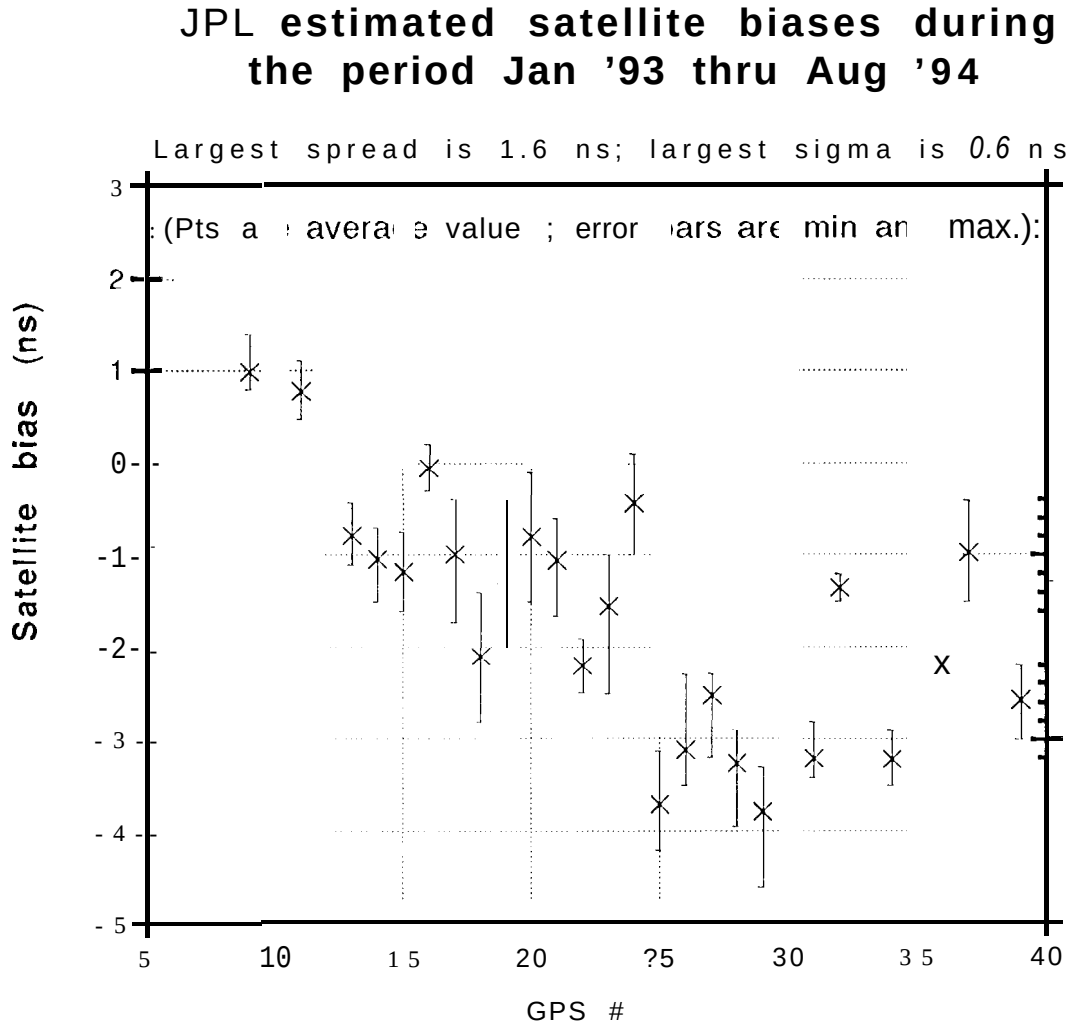

Figure 6 Plot of the mean of the estimates for each satellite bias for seven 10-12 day periods spanning Jan. 199310 Aug. 1994. The error bars represent, not the standard deviation, but the total variation of the seven estimates during the 20 month period. The largest variation is 1.6 ns for GPS #19, while the largest standard deviation is 0.6 ns for GPS #29.